

Production of a severe cystic fibrosis mutation in mice by gene targeting

Rosemary Ratcliff¹, Martin J. Evans¹, Alan W. Cuthbert², Lesley J. MacVinish², Diane Foster¹, Janice R. Anderson³ & William H. Colledge¹

We have used gene targeting in embryonic stem cells to introduce an *HPRT* mini-gene into the coding sequence of the murine cystic fibrosis gene (*cftr*). This insertion introduces a termination codon in frame with the *cftr* coding sequence to terminate prematurely the CFTR protein within the first nucleotide binding domain. Animals homozygous for the *cftr* disruption fail to thrive and display a range of symptoms including meconium ileus, distal intestinal obstructions, gastrointestinal mucus accumulation and blockage of pancreatic ducts. The animals also show lacrimal gland pathology. Tracheal and caecal transepithelial current measurements demonstrate the lack of a cAMP activatable Cl⁻ channel. These animals will prove useful for the evaluation of new therapeutic drugs and gene therapy strategies.

¹Wellcome/CRC Institute of Cancer and Developmental Biology and Department of Genetics, University of Cambridge, Tennis Court Road, Cambridge CB2 1QR, UK

²Department of Pharmacology, University of Cambridge, Tennis Court Road Cambridge CB2 1QJ, UK

³Department of Histopathology, Addenbrookes Hospital, Hills Road, Cambridge CB2 2QQ, UK

Correspondence should be addressed to W.H.C.

Cystic fibrosis (CF) is a fatal autosomal recessive genetic disorder affecting about 1 in 2,000 Caucasians. The disorder is characterized by hypersecretion of mucus in the lungs, intestinal obstructions, reduced ability to digest and absorb duodenal contents due to pancreatic insufficiency, male sterility and elevated salt levels in the sweat¹. The gene mutated in CF, the cystic fibrosis transmembrane conductance regulator (*CFTR*) gene, encodes a Cl⁻ channel that is regulated by cAMP-dependent protein kinase phosphorylation and nucleoside triphosphate binding². Over 200 mutations have been described within the human *CFTR* gene including missense, nonsense, splice site alterations, frame shift deletions and insertions³. The most common mutation, present in about 75% of CF patients, is a three base pair deletion in exon 10 resulting in loss of phenylalanine 508 ($\Delta F508$)^{4,5}.

An animal model for CF would be useful for several reasons: (i) To understand the pathology and pathophysiology of the disorder. (ii) To develop new therapeutic compounds aimed at alleviating the symptoms of CF (iii) To test gene therapy strategies and develop efficient gene delivery systems. (iv) To manipulate the genetic background of the animals to assess genetic effects on the penetrance level of the disorder.

We describe here the production of a new *null* allele in the mouse *cftr* locus and the phenotype of homozygous mutant animals. Our preliminary observations have been reported previously⁶. Independently, two other groups have also generated animals homozygous for a *cftr* disruption in exon 10. Snouwaert *et al.* (University of North Carolina), used a replacement type targeting construct to introduce a double *neo^r* gene into the *cftr*

locus in ES cells (UNC mutation)⁷ while Dorin *et al.* (University of Edinburgh) introduced a single *neo^r* gene through an insertion event (EDI mutation)⁸.

The mice that carry the replacement arrangement (UNC mutation) have the more severe phenotype and most die within 30 days after birth from intestinal blockages caused by hyper-accumulation of mucus. In addition, the animals fail to thrive, suffer from meconium ileus and show alterations of mucus and serous glands and do not show a cAMP stimulated Cl⁻ channel activity in epithelial cells^{7,9}. In contrast, the EDI animals show no overt clinical disease and develop only minor pathological changes in a sub-set of animals⁸.

Our homozygous mutant animals (CAM mutation) show a remarkably similar phenotype to the UNC animals, notably a failure to thrive, meconium ileus, distal intestinal obstructions, gastrointestinal mucus accumulation, and lack of a cAMP activatable Cl⁻ channel. However, we also find blockage of pancreatic ducts in some CAM CF animals and lacrimal gland pathology, changes not yet reported for CF mice.

Generation of mice carrying a disrupted *cftr* allele

Embryonic stem (ES) cells previously mutated at the *hpvt* locus were targeted with a replacement construct which, upon homologous recombination, results in the addition of 88 amino acids followed by a termination codon after the codon for arginine 487 of *cftr*. HPRT function is restored. This mutation therefore disrupts the *cftr* locus in exon 10 (Fig. 1a).

Two of the targeted lines were injected into C57Bl/6 host blastocysts and chimaeric animals were derived (Table 1a). Both targeted cell lines gave rise to partial germline

chimaeras as judged by transmission of agouti coat colour. Polymerase chain reaction (PCR) and Southern blot analysis of tail DNA was used to identify F_1 pups heterozygous for the disrupted *cftr* locus. Heterozygote F_1 animals were intercrossed to generate homozygous CF offspring (Table 1b). Both male chimaeras and F_1 heterozygote animals were fertile and the expected 1:1 segregation from the F_1 animals was observed (Table 1b).

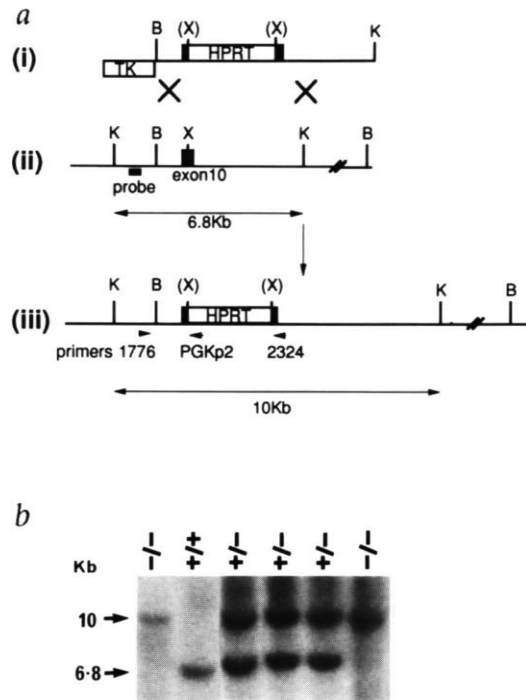


Fig. 1 In order to create a variety of mutations in the mouse *cftr* gene we adopted a strategy of double replacement which should enable construction of $\Delta F508$ as well as a number of other different mutations in exon 10 (refs 32, 33). The first stage of this replacement gene targeting strategy produces a disruption in the normal gene which should in itself provide a useful model mutation. The targeting strategy is shown in (a). The targeting construct, pCF-B(hprt)tk, contains an *HPRT* mini-gene cloned into the *XmnI* site within *cftr* exon 10. a, (i) Schematic representation of targeting vector. (ii) Arrangement of endogenous *cftr* exon 10 and surrounding sequence. For PCR screening of ES clones, primers 1776 and PGKp2 amplified a 1.2 kb DNA segment only when *HPRT* was present at the target locus. For PCR analysis of tail genomic DNA, the primer combination 1776/PGKp2 amplified the 1.2 kb fragment from DNA of either heterozygous or homozygous CF animals. The 1776/2324 combination amplified only non-disrupted endogenous exon 10 sequence, therefore giving a 1.2 kb band in normal and heterozygous animals (results not shown). For Southern analysis of genomic DNA from ES clones and tails, a 900 bp probe (*KpnI*-*HindIII* fragment) was derived from sequence upstream of that present in the targeting construct (results shown Fig 1b). *HPRT*, hypoxanthine phosphoribosyl transferase gene; TK, thymidine kinase gene; B, *Bam*HI; K, *Kpn*I; X, *Xmn*I, deleted when in brackets. (iii) Arrangement of exon 10 region following double crossover replacement of the endogenous *cftr* locus by the *HPRT*-containing vector sequence. The PGKtk gene is lost on recombination, bestowing gancyclovir resistance. b, Southern blot analysis demonstrating homozygous wild-type (+/+), carrier (+/-) and homozygous mutant (-/-) offspring in the F_2 generation derived by crossing F_1 carriers for the *cftr* disruption. Genomic DNA was prepared from tails, digested with *Kpn*I and size fractionated by agarose gel electrophoresis. The probe is external to the targeting construct and hybridizes to a 6.8 kb *Kpn*I fragment from the wild-type *cftr* locus and a 10 kb *Kpn*I fragment from the mutated *cftr* locus.

The genotypes of the pups born in the F_2 generation is not statistically different from the expected 1:2:1 ratio of wild type:carrier:homozygote CF which indicates that there is little, if any, prenatal lethality associated with homozygosity of this mutant allele (Table 1b). Figure 1b shows a typical Southern analysis identifying wild type (+/+), carrier (+/-), and homozygous mutant (-/-) animals in the F_2 offspring.

Phenotype of CF mice

Post-natally many homozygote mutant pups fail to thrive and approximately 80% were found dead between two and five days after birth (Fig. 2). The mortality of homozygous animals was significantly greater than expected ($P < 0.005$ by χ^2 analysis) and this early death is highly correlated with lack of a wild-type *cftr* allele (Table 1b). Dissection of these animals revealed that the majority had breathed and suckled prior to death. Most of the animals were found with inspissated meconium obstructions in the ileum region of the small intestine⁶. Death of most of these animals was caused by severe peritonitis.

Although the majority of homozygous mutant pups died within a few days of birth, some survived to later developmental stages. In general, however, these animals also failed to thrive and appeared runted compared with their litter mates. CF animals are typically half the weight of their normal litter mates throughout their life. These animals go through a second period of mortality at around 21 days after birth (Fig. 2) which corresponds to the time when they are first ingesting solid food. The older animals also suffer from intestinal blockages manifest both in the small and large intestine although the latter are somewhat more common⁶. This second stage blockage of the intestine is similar in onset to the distal intestinal obstruction syndrome observed in older CF patients¹⁰.

Pathohistology

Intestine. Histological examination of the small intestine from our CF mice showed that most of the crypts of Lieberkühn were severely dilated (Fig. 3b) compared with equivalent aged wild-type mice (Fig. 3a). Periodic acid Schiff (PAS) staining of sections through the jejunum and ileum regions of the small intestine demonstrated that the crypts were filled with excessive mucus (Fig. 3c) that often

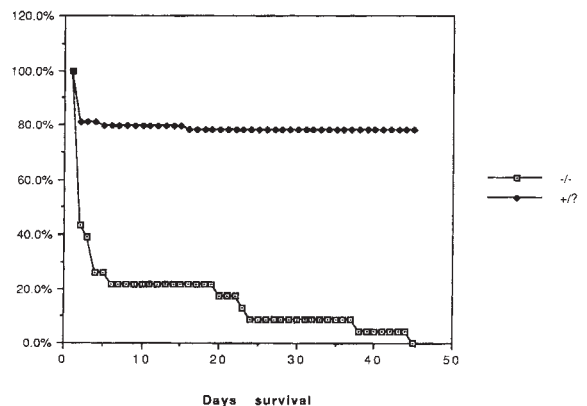


Fig. 2 Survival rates of CF homozygous animals compared with the combined group of heterozygous carrier and wild-type siblings.

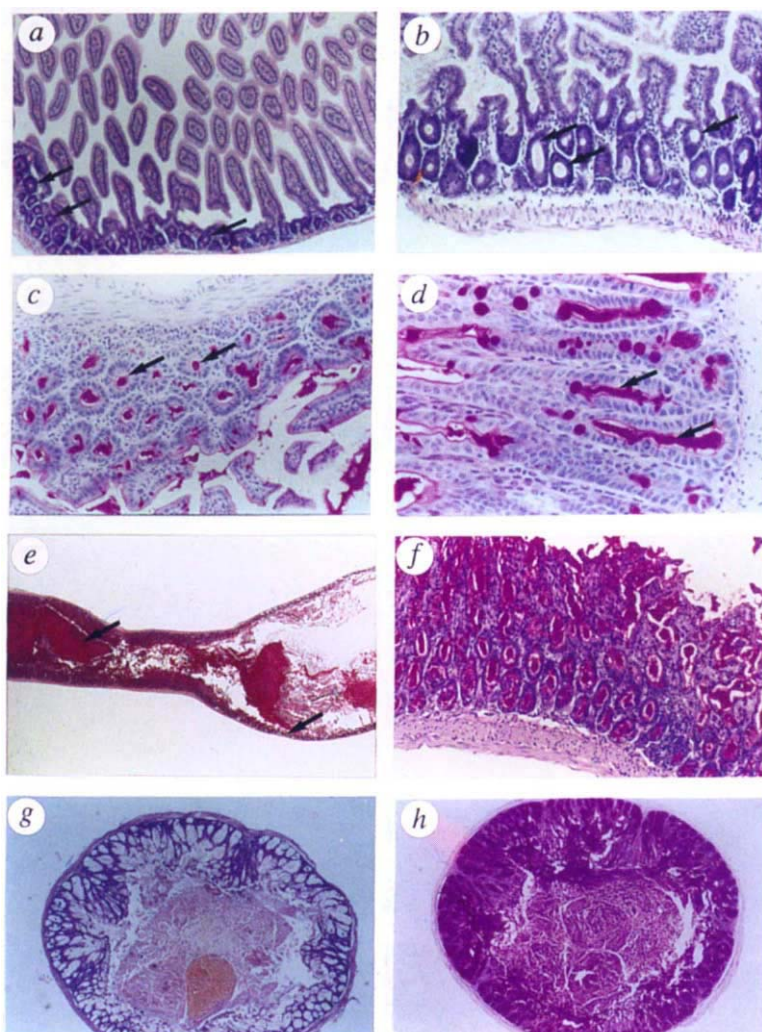
Table 1 Construction and breeding records of chimaeras and F₁ animals transmitting the disrupted *cftr* allele

a Chimaera construction and germline transmission						
Clone	Blastocysts injected	Mice born	Female chimaera	Male chimaera	Germline males	
CF21.1	21	8	0	3	3/3	
CF21.11	44	16	3	7	4/7	

b F ₁ intercross to give rise to homozygous animals						
Genotype	Alive		Dead		Total	Expected (1:2:1)
	obs	exp*	obs	exp*		
+/+	22	14.5	5	10.5	27	25
+/-	34	29	10	21	44	50
-/-	2	14.5	27	10.5	29	25

$\chi^2 = 15.52$ $p < 0.005$	$\chi^2 = 34.57$ $p < 0.005$	$\chi^2 = 1.52$ not significant
---------------------------------	---------------------------------	------------------------------------

The observed numbers of offspring born (dead and alive) were compared with an expectation for a overall 1:2:1 mendelian ratio and the viability was compared with an expectation of random lethality not associated with the genotype (*). χ^2 values show no significant difference from expectation of Mendelian ratio indicating that there is no prenatal lethality associated with the mutation but later death is highly correlated with genotype ($p < 0.005$).



extended the complete length of the crypt (Fig. 3d). A transverse section through a jejunal blockage showed the obstruction to be composed of an inspissated amalgam of food material and mucus (Fig. 3e). Considerable distention of the intestine was observed proximally to the blockage and within the distended region the majority of the intestinal villi were severely atrophic and in places necrotic (Fig. 3f). Crypt distention and mucus hypersecretion were also observed in the colon. (Fig. 3g,h). Overproduction of mucus in the intestine was a consistent feature in all CF mice analysed irrespective of age ($n = 10$). Mucus abnormalities were found in animals as young as 24 h, consistent with a causative role in the development of meconium ileus in these young animals.

Lungs. The major cause of morbidity in CF patients is through respiratory failure following lung destruction by repeated microbial colonization of the airways¹. CF lungs are characterized by thick mucus secretions that promote such infections. To assess how closely the CF mice would mimic the lung pathology changes observed in CF patients, histological sections were prepared from neonates as well as 4 week old animals. No pathological accumulation of mucus was observed in lung airways from any CF animal analysed ($n = 10$, Fig. 4a).

Pancreas. The majority of CF patients suffer progressive deterioration of pancreatic function associated with blockage of the secretory ducts resulting in failure to secrete pancreatic enzymes¹¹. Ductal obstruction is associated with gradual pancreatic atrophy and fibrosis of the exocrine parenchyma. Although pancreatic *cftr* expression is low in rodents compared with humans, histological examination of CF mice showed dilatation and blockage of several small pancreatic ducts in five out of ten CF animals (Fig. 4c). The material in the lumen stained lightly with PAS diastase and had a structured appearance indicating that the staining was not artifactual. Similar staining was never observed in normal mice. Pancreatic abnormalities were not observed (Fig. 4b) in animals younger than 17 days and even in affected animals the lesions were focal. In some CF animals, occasional vacuolated acinar cells were found (data not shown). These may be similar to the enlarged acini reported to be present in some UNC CF animals.

Lacrimal glands. Several CF animals developed eye infections and were prone to persistent eye closure prompting us to examine lacrimal glands from the CF animals. A comparison of lacrimal glands from wild-type (Fig. 4d) with CF (Fig. 4e) showed acinar dilatation in the

Fig. 3 Gastrointestinal histopathology in CF animals. **a**, Transverse section of small intestine from a normal 21 day old mouse showing villous architecture and the appearance of crypts of Lieberkühn (H&E). **b–d**, Transverse sections of small intestine from a 21 day old CF mouse showing crypts of Lieberkühn distended with mucus (arrowed). (**b,c**, H&E; **d**, PAS diastase). **e**, Longitudinal section of small intestine from a CF mouse showing inspissated mucus distending the bowel lumen and causing villous atrophy (arrowed) of the intestinal mucosa (PAS diastase). **f**, Higher magnification of **e** illustrating distended crypts filled with mucus (PAS diastase). **g,h**, Transverse sections of large intestine from CF mouse showing crypts filled with mucus (**g**, H&E; **h**, PAS diastase).

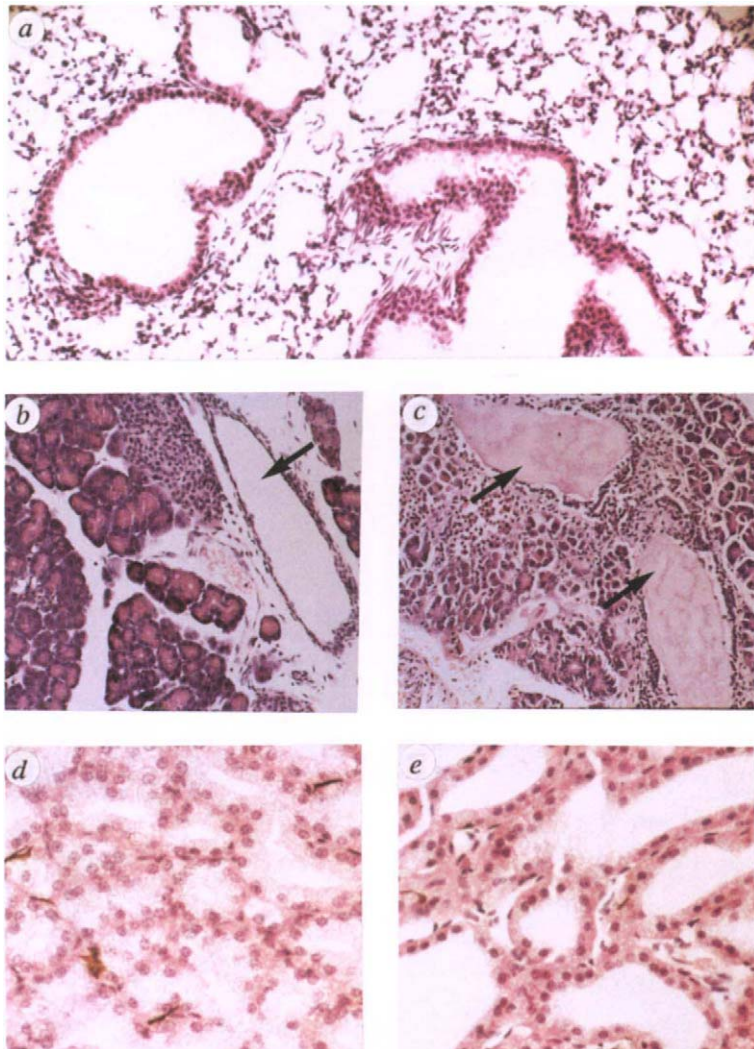


Fig. 4 Lung, pancreas and lacrimal gland histopathology. *a*, Section from lung of a homozygous CF animal showing small bronchi with normal epithelial lining and normal surrounding alveoli. *b*, Pancreas from a normal animal showing patent small duct (arrowed) adjacent to an islet of Langerhans and surrounded by normal exocrine tissue (H&E). *c*, Pancreas from a homozygous CF animal showing pancreatic ducts (arrowed) filled with secretion (PAS diastase). *d*, Lacrimal gland from a heterozygous animal showing normal appearance of closely packed small acini. Interstitial cells with brown cytoplasm are melanocytes (H&E). *e*, Lacrimal gland from a CF animal showing acinar dilation (H&E).

back pressure that results in acini dilation. Lacrimal gland abnormalities were found in most (5/7) CF mice examined irrespective of identification of eye problems. A similar pathology has not yet been reported in either the UNC or EDI CF mice.

Characteristics of transepithelial transport *in vitro*

Electrogenic transepithelial ion transport was measured in tracheal and caecal epithelia as short circuit current (SCC). Data from wild types (+/+) and carriers (+/-) have been pooled as no significant differences between these groups have been found with the present numbers (Tables 2 and 3). Although transepithelial potentials of murine tracheal epithelium *in vitro* has been reported¹² we have attempted to measure the quantitative relationships of different transport processes by voltage clamping at zero potential and using pharmacological agents to eliminate or stimulate various processes. Characteristics of the processes in normal tracheal epithelium are given in Table 2. Some 50% of the basal current was due to sodium absorption, and was specifically removed by adding amiloride to the apical bathing solution. Forskolin, to increase cAMP content, increased SCC by the same extent, whether or not amiloride had been added. A23187, a calcium ionophore, also increased SCC either alone or on the plateau current following forskolin (data not shown). Near complete inhibition of the SCC increases following forskolin or forskolin plus A23187, after amiloride, was obtained when the Na⁺ K⁺ 2Cl⁻ co-transport inhibitor, frusemide, was added to the basolateral bathing solution. Only 3 CF animals reached sufficient size to give satisfactory tracheal preparations, and their amiloride and forskolin-sensitive SCCs were significantly reduced. Amiloride sensitive SCC was $2.6 \pm 0.2 \mu\text{A cm}^{-2}$ ($n = 3$) compared to $11.1 \pm 2.2 \mu\text{A cm}^{-2}$ ($n = 6$) in controls ($P < 0.005$, Student's *t*-test). Forskolin sensitive SCC was only $4.8 \pm 1.2 \mu\text{A cm}^{-2}$ ($n = 3$) and significantly less than the value for the pooled controls ($20.0 \pm 1.9 \mu\text{A cm}^{-2}$, $n = 8$, $P < 0.001$) or carriers (+/-) ($18.5 \pm 4.6 \mu\text{A cm}^{-2}$, $n = 4$, $P < 0.05$ one-tailed).

Normal caecal epithelia showed increases in SCC to forskolin, ATP (applied apically) and carbachol (applied basolaterally) but not to A23187. Furthermore responses to amiloride were barely discernible. Some 80–90% of the forskolin-induced current was eliminated by frusemide applied basolaterally. Glucose was used by the UNC group⁹ to stimulate Na⁺ dependent glucose uptake, and hence an absorptive SCC, in otherwise insensitive CF intestinal tissues. In our hands, responses to glucose added to tissues bathed in glucose-free medium were unreliable, not all tissues responding even when several pieces were from the same animal.

Caecae varied considerably in size and were very small

latter although there was no obvious accumulation of mucus. It is possible that blockages might be confined to the larger more distal lacrimal ducts thus producing a

Table 2 Characteristics of electrogenic ion transport in murine tracheal epithelium (8 +/+ and 4 +/-)

Drug treatment	SCC ($\mu\text{A cm}^{-2}$)	Sample size (<i>n</i>)
Basal	20.9 ± 2.3	12
Amiloride-sensitive	11.1 ± 2.2 ($57.1 \pm 19.2\%$ inhibition)	6
Forskolin-sensitive	20.0 ± 1.9	12
Before amiloride	17.3 ± 1.5	6
After amiloride	22.7 ± 3.3	6
Forskolin-sensitive		
In +/+	20.7 ± 1.9	8
In +/-	18.5 ± 4.6	4
Frusemide inhibition of response to forskolin (+ A23187) in presence of amiloride	$93.2 \pm 6.5\%$ inhibition	6

Drugs were used at the following concentrations: Forskolin, 10 μM and A23187, 1 μM , were applied to both sides of the tissue; amiloride, 100 μM was applied only to the apical side; frusemide, 1 mM was applied only to the basolateral side of the tissue.

The concentrations of drugs used were judged sufficient to cause maximal stimulation or inhibition of processes involved in ion transport.

Table 3 Characteristics of electrogenic ion transport in murine caecal epithelium, normal and CF

Drug treatment	SCC ($\mu\text{A cm}^{-2}$)	Sample size (<i>n</i>)
a 60 mm²		
Basal	54.8 ± 8.2	14
Forskolin-sensitive	205 ± 43.5	14
Frusemide inhibition	(84.0 ± 5.1%)	14
CF basal	25.9	2
CF forskolin-sensitive	0.0	2
b 20 mm²		
Basal	23.9 ± 10.5	7
Forskolin-sensitive	39.0 ± 6.9	7
Frusemide inhibition	(92.7 ± 9.8%)	7
CF basal	7.6 ± 1.1	3
CF forskolin-sensitive	0.7 ± 0.3	3
c 4 mm²		
Basal	14.6 ± 5.0	4
Forskolin-sensitive	14.3 ± 3.5	4
Frusemide inhibition	(107.9 ± 23.5%)	4
CF basal	1.9	2
CF forskolin-sensitive	0.6	2

For the 7 CF epithelia the mean forskolin response was $0.5 \pm 0.3 \mu\text{A cm}^{-2}$ ($n = 7$). This value is significantly different ($P < 0.001$) from that in normal epithelia of 4 mm^2 area, that is, $14.3 \pm 3.5 \mu\text{A cm}^{-2}$ ($n = 4$). Forskolin, 10^{-6} M , was added to both apical and basolateral baths, while frusemide (1 mM) was added only to the basolateral side. Controls consisted of 18 $+/+$ and 7 $+/-$ mice.

especially in CF mice. Figure 5a–c shows responses from epithelial sheets of 60 mm^2 , 20 mm^2 and 4 mm^2 . In each case, the lower trace shows responses of CF epithelia compared to normal tissue shown in the upper tracings. Statistical data for this group is given in Table 3, showing that the CF phenotype virtually abolishes the response to forskolin. The responses in normal epithelia are considerably less when converted to $\mu\text{A cm}^{-2}$ for small areas. This is inevitably due to the ratio of circumference to area leading to the greater edge damage that occurs in mounting small tissues. For the majority of the data presented in Table 3 the phenotype was deduced before the genotype was determined. They corresponded in all instances.

In 4 out of 5 CF caecal epithelia where frusemide was applied basolaterally, an increase in SCC was observed (Fig. 5a,b). The reasons for this are unclear, but it provides a useful indicator of viability. This increase in SCC develops slowly and may be masked in normal epithelia because of the rapid fall associated with blockage of Cl^- secretion.

Discussion

Genotype/phenotype comparisons¹³ have shown that nonsense mutations within the human *CFTR* gene are associated with severe phenotypes. In particular, Q493X which terminates the polypeptide within exon 10 causes, when allelic with ΔF508 , severe pancreatic insufficiency. In a proportion of such severely affected human cases one of the earliest pathological manifestations is blockage of the gut by viscous contents, known as meconium ileus. The early death of the majority of homozygous mice observed here is due to such a condition. However, whereas some 80% of the CF mice develop meconium ileus, only about 10% of CF patients are present with these symptoms at birth¹⁴. The reason for this difference is unknown. It is noteworthy, however, that the incidence of meconium

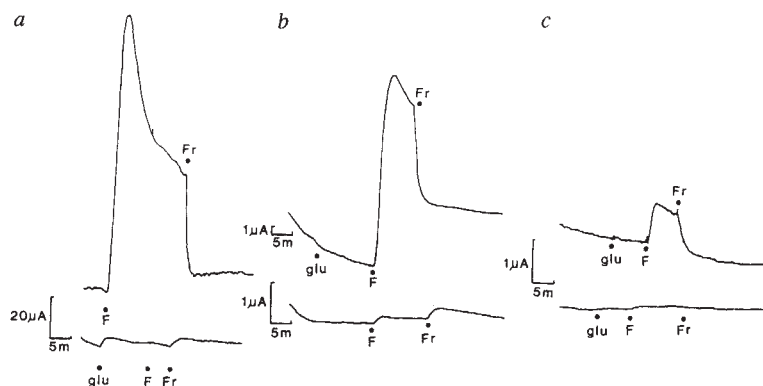
ileus was found to be over-represented in patients who had the $\Delta\text{F508}/\text{G542X}$ genotype¹³. If a severe mutation (ΔF508) combined with a termination mutation in the first NBD increases the risk of meconium ileus then perhaps homozygosity for a *null* mutation terminating in the first NBD, as in the case of our animals, will be almost invariably associated with meconium ileus. To our knowledge, no patients have been reported as carrying two NBD 1 termination mutations. A corollary of this hypothesis is the prediction that ΔF508 homozygous mice will show a lower incidence of meconium ileus than either our *null* CF mice or the UNC mice.

As in the human syndrome, not all neonatal CF mice develop meconium ileus but they are prone to a second stage blockage at a later time akin to distal intestinal obstruction syndrome in man¹⁰. The F_2 mice reported here are on a genetically diverse background because the original 129 strain ES-cell-based allele has been outcrossed to both C57Bl/6 inbred and MF1 outbred stocks. In order to retain the allele on a known genetic background we have also crossed the original chimaeric mice to 129 strain females. This should allow us to examine the influence of genetic background on the expression and penetrance of this mutation.

While our older CF animals show histological evidence of slight pancreatic pathology, this is not considered severe enough to alter significantly pancreatic exocrine function. The appearance of blocked pancreatic ducts suggests that, as in human CF patients, there might be a defect in the secretion of Cl^- and bicarbonate ions into the pancreatic ducts leading to precipitation of calcium salts and proteins. A reduction in pancreatic bicarbonate ion secretion results in a failure to neutralize the gastric juices entering the duodenum from the stomach. The acid pH within the duodenal lumen inactivates pancreatic enzymes thus reducing food digestion and assimilation and perhaps contributing to the runting observed in the CF animals. In addition, acidification of the small intestine can promote the precipitation of bile salts. Thus the failure to thrive of our CF mice might also be caused in part by an inability to form sufficient bile salt/fatty acid micelles as well as a potential reduction in absorption capacity due to the thick mucus coating of the intestinal villi.

Our animals show a very similar phenotype to the UNC animals whilst the EDI mice have a less severe phenotype. The reasons for these phenotypic differences are still to be clearly resolved. It has been suggested that the type of genetic alteration (replacement versus insertion) engineered into *cftr* may affect the extent to which the anticipated *null* mutation is leaky. Alternatively, the phenotypic differences could result from the different genetic backgrounds onto which the *cftr* mutations have been introduced. The UNC mutation has been crossed onto three different inbred strains while the EDI mutation has been carried in an essentially outbred population. We have maintained our mutation on an outbred genetic background in a similar fashion to the EDI mutant. This suggests that the genetic background (that is inbred versus outbred), while it may still play a role in the penetrance levels associated with the symptoms, is less important in determining the overall severity of the disorder than the genetic alteration itself. If the insertion mutation in the EDI animals can undergo transcriptional read through these transcripts may be alternatively spliced to remove the mutation thus generating low but physiologically

Fig. 5 SCC records from caecal epithelia. Epithelial areas were 60 mm² (a), 20 mm² (b) and 4 mm² (c). In each pair of traces the upper record is from tissues from normal mice while the lower traces are from tissues from CF mice. When glucose (glu) was added the tissues had been mounted initially in glucose-free medium and a small volume of glucose solution was added to restore the normal concentration. In each experiment forskolin (F), 10 µM, was added to the solution bathing both sides of the tissue. After the responses had peaked frusemide (Fr), 1 mM, was added to the basolateral bathing solution. Where a single calibration is shown by a pair of records it applies to both.



relevant wild-type CFTR function. An insertion within the *N-myc* coding sequence has been shown to give rise to a full length functional mRNA at a low level by exon splicing¹⁵.

Our CF animals lack a cAMP activatable Cl⁻ channel in both the tracheal and caecal epithelia. While the SCC responses to forskolin in CF caecae were virtually abolished (inhibition >96%) some response was still obtained in CF tracheae (~25% of control). The differential effect in these two tissues requires explanation and it needs to be demonstrated that the SCC responses represent Cl⁻ secretion. Clearly there is more than one pathway for Cl⁻ secretion in airway epithelia since the Ca²⁺ dependent, but not the cAMP dependent response is preserved in CF airway epithelial cells¹⁶⁻¹⁸ and in normal epithelial cells treated with CFTR antisense oligonucleotides¹⁹. In CF epithelial cells, failure to respond to cAMP is apparently due to a failure of intracellular protein trafficking²⁰⁻²², ΔF508 CFTR failing to reach the plasma membrane, yet in these homozygous mutant murine tracheae, where it is unlikely that CFTR is produced, small responses to cAMP are recorded. The ORDIC Cl⁻ channel, which is sensitive to the cAMP/PKA cascade²³, might act as an alternative route for Cl⁻ efflux from the cell, although it is an unlikely normal function. Nevertheless, hyperpolarization of the apical membrane with amiloride increases the likelihood of Cl⁻ efflux by this route. However if the recently resurrected proposal that ORDIC channels are also deficient in CF²⁴ is proven, then the residual forskolin responses in the CF murine tracheae will require further explanation.

There can be little doubt that the SCC responses recorded here are due to electrogenic Cl⁻ secretion. Sufficient amiloride to block sodium absorption in the trachea does not affect, indeed marginally increases (Table 2) the size of the responses to forskolin. In both trachea and caecum the responses to Cl⁻ secretory agonists are ~90% inhibited by frusemide, applied basolaterally to block the Na⁺K⁺2Cl⁻ cotransporter, responsible for Cl⁻ uptake into the cells.

Human CF airway epithelium shows an increased ability to absorb sodium²⁵⁻²⁷ although it is unclear whether this is due to an increased number of apical Na⁺ channels or to increased open state probability. In consequence, the amiloride-sensitive SCC is greater in CF epithelia than in normals. This phenomenon was not observed in the murine CF tracheal epithelia in this study. Possibly enhanced Na⁺ absorption is a slow adaptation phenomenon in man and would appear in mice if they survived the immediate neonate period. Alternatively,

effects on Na⁺ and ORDIC channels in CF may be related to the disruption of intracellular protein trafficking, not a likely event with a *null* mutation in CF mice.

The caecal epithelium provides a more simple test system than the trachea. First it shows no appreciable sodium absorbing capacity and secondly, the epithelial area available, even in neonate mice is greater than with trachea. Finally, the caecum responds to forskolin with a Cl⁻ secretory current which is blocked by frusemide, applied basolaterally. Responses to forskolin were dependent upon area, because of edge damage (Table 3) but responses to forskolin were not seen in CF epithelia of any area. CF epithelia showed a SCC increase to frusemide and while this is as yet unexplained, the combination of a failure to respond to forskolin and an increase in current to frusemide is a useful signature for CF caecal epithelia in the mouse.

Our animal model shows some of the classic symptoms of CF, namely failure to thrive, intestinal mucus obstructions and some pancreatic abnormalities. These animals can therefore be used to develop new pharmacological agents for the treatment of CF, in particular compounds that alleviate some of the gastrointestinal problems associated with CF. The animals also show pathology that has not been reported in humans, that is lacrimal gland alterations. Epithelial cells from both the trachea and the caecum fail to generate a Cl⁻ channel conductance in response to increased intracellular cAMP concentrations. The availability of animals with a very low Cl⁻ channel activity should provide a sensitive system for detecting restoration of the low conductance CFTR channel after various gene therapy strategies have been tried.

Methodology

Construction of *cftr* targeting plasmid. The targeting vector pCF-B(hprt)tk contains a 5.4 kb *Bam*HI-*Kpn*I fragment of mouse *cftr* sequence, surrounding the 180bp exon 10. This was subcloned into a pUC18 vector from a λXT1 clone derived from a mouse 129 strain library²⁸. A 3.2 kb human *HPRT* minigene²⁹ was inserted into the *Xmn*I site in exon 10, and a *tk* gene ligated to the 5' end of the homology region. Both markers are driven by a PGK (phosphoglycerate kinase) promoter³⁰. The vector was linearized at the 3' *Kpn*I site and used to transform the *hprt* ES cell line TG4³¹. The TG4 line is close in origin to the construct, but not strictly isogenic

ES cell culture and selection. ES cells were cultured on mitotically inactivated STO-feeder cells. Cells were trypsinized and electroporated with 10 µg of linearized targeting vector. 1 × 10⁷ cells ml⁻¹ in PBS were electroporated using a BioRad Gene Pulser at 250V/0.4 cm, 500 µF. The ES cells were allowed to recover for 5 min at room

Acknowledgements

We are grateful to the CF Trust and the Wellcome Trust for their support of this work and the animal house staff for excellent husbandry. Also all members of the Evans' laboratory. We thank Professor Bob Williamson and Brandon Wainwright for providing the cfr⁺ clone.

temperature before plating at 1×10^6 cells per 9 cm dish. HAT selection was applied 24 h later followed by gancyclovir (2 mM) selection after an additional 24 h. Colonies were picked 10–14 days after electroporation and screened for targeting events by Southern blot and PCR as described³³. The average enrichment after selection in HAT/gancyclovir was 10-fold. Four positive clones were identified from 19 HAT⁺/ganc⁺ clones in one experiment giving a targeting frequency from this electroporation of 3.5% of all HAT⁺ colonies. The targeting frequency was found to vary from one electroporation to the next.

Histology. Mice were killed by exposure to 100% CO₂. The thorax and abdomen were opened and after removal of the trachea the whole body was immersed in 4% phosphate buffered formalin. After adequate fixation the thoracic and abdominal organs, the eyes and salivary glands were carefully dissected. Organs were embedded in paraffin wax and 5 µm sections were cut and stained with haematoxylin and eosin and Periodic Acid Schiff with diastase.

Electrogenic transport measurements. Tracheae were dissected

from mice, killed by exposing to 100% CO₂, cleaned and cut longitudinally along the dorsal surface. Pieces, around 2.5 mm square, were placed under microscopic control in specially constructed Ussing chambers, designed to preserve the curvature of the tissue. Mouse caecae were dissected out, opened along the mesenteric border and cleaned by gentle wiping with tissue soaked in KHS. No attempt was made to strip the muscle coats. Transepithelial potential was measured with fine polythene tubes filled with Krebs solution. These led via calomel cells to the input stage of a WPI dual voltage clamp. Current was passed via Ag/AgCl electrodes and agar-filled KCl bridges at a point in the chambers 5 cm from the tissue. The tips of the potential electrodes were within 1 mm of the tissue surface. Short circuit currents (SCC) were recorded by voltage clamping the tissue at zero potential. Each side of the tissue was bathed with 20 ml of KHS which was continually circulated by a gas lift. The bathing solutions were maintained at 37 °C and continuously bubbled with 95% O₂/5% CO₂. The Krebs Henseliet solution (KHS) had the following composition (mM): NaCl 118, KCl 4.7, CaCl₂ 2.5, MgSO₄ 1.2, KH₂PO₄ 1.2, NaHCO₃ 25 and glucose 11.1. The solution had a pH of 7.4 at 37 °C when gassed with 95% O₂/5%CO₂.

Received 4 November 1992; accepted 11 January 1993.

- Hodson, M., Norman, A.P. & Batten, J.C. eds *Cystic Fibrosis* (Bailliere Tindall, London, 1983).
- Anderson, M.P. *et al.* Nucleoside triphosphates are required to open the CFTR chloride channel. *Cell* **67**, 775–784 (1991).
- Tsui, L.-C. The spectrum of cystic fibrosis mutations. *Trends Genet.* **8**, 392–398 (1992).
- Riordan, J.R. *et al.* Identification of the cystic fibrosis gene: cloning and characterisation of complementary DNA. *Science* **245**, 1066–1073 (1989).
- Kerem, B. *et al.* Identification of the cystic fibrosis gene: genetic analysis. *Science* **245**, 1073–1080 (1989).
- Colledge, W.H., Ratcliff, R., Foster, D., Williamson, R. & Evans, M.J.: Cystic fibrosis mouse with intestinal obstruction. *Lancet* **340**, 680 (1992).
- Snouwaert, J.N. *et al.* An animal model for cystic fibrosis made by gene targeting. *Science* **257**, 1083–1088 (1992).
- Dorin, J.R. *et al.* Cystic fibrosis in the mouse by targeted insertional mutation. *Nature* **359**, 211–215 (1992).
- Clarke, L.L. *et al.* Defective epithelial chloride transport in a gene targeted mouse model of cystic fibrosis. *Science* **257**, 1125–1128 (1992).
- Hunton, D.B., Long, W.K. & Tsumagari, H.Y. Meconium ileus equivalent: an adult complication of fibrocystic disease. *Gastroenterology* **50**, 99–107 (1966).
- Hadorn, B. *et al.* Quantitative assessment of exocrine pancreatic function in infants and children. *J. Pediatr.* **73**, 39–48 (1968).
- Smith, S.N., Alton, E.W.F. & Geddas, D.M. Ion transport characteristics of the murine trachea. *Clin. Sci.* **82**, 667–672 (1992).
- Kristidis, P. *et al.* Genetic determination of the exocrine pancreas function in cystic fibrosis. *Am. J. hum. Genet.* **50**, 1178–1184 (1992).
- Donnison, A.B., Shwachman, H. & Gross, R.E. A review of 164 children with meconium ileus seen at the Children's Hospital Medical Centre, Boston. *Pediatrics* **37**, 833–843 (1966).
- Moens, C.B., Auerbach, A.B., Conlon, R. A., Joyner, A.L. & Rossant, J. A targeted mutation reveals a role for N-myc in branching morphogenesis in the embryonic mouse lung. *Genes Devel.* **6**, 691–704 (1992).
- Willumsen, N.J. & Boucher, R.C. Activation of an apical Cl⁻ conductance by Ca²⁺ ionophores in CF airway epithelia. *Am. J. Physiol.*, **256**, 226–233 (1989).
- Wagner, J.A. *et al.* Activation of chloride channels in normal and cystic fibrosis airway epithelial cells by multifunctional calcium/calmodulin dependent protein kinase. *Nature* **349**, 793–796 (1991).
- Anderson, M.P. & Welch, M.J. Calcium and cAMP activate different chloride channels in the apical membrane of normal and cystic fibrosis epithelia. *Proc. Natl. Acad. Sci. U.S.A.* **88**, 6003–6007 (1991).
- Wagner, J.A., *et al.* Antisense oligodeoxynucleotides to the cystic fibrosis transmembrane conductance regulator inhibit cAMP activated but not calcium-activated chloride currents. *Proc. natn. Acad. Sci. U.S.A.* **89**, 6785–6789 (1992).
- Chang, S.H. *et al.* Defective intracellular transport and processing of CFTR is the molecular basis of most cystic fibrosis. *Cell* **63**, 827–834 (1990).
- Gregory, R.J. *et al.* Maturation and function of cystic fibrosis transmembrane conductance regulator variants bearing mutations in putative nucleotide binding domains 1 and 2. *Molec. cell Biol.* **11**, 3886–3893 (1991).
- Kartner, N., Augustinos, O., Jensen, T.J., Naismith, A.L. & Riordan J.R. Mislocalization of ΔF508 CFTR in cystic fibrosis sweat gland. *Nature Genet.* **1**, 321–327 (1992).
- Henderson, R.M., Ashford, M. L. J., MacVinish, L. J. & Cuthbert A. W. Chloride channels and anion fluxes in a human colonic epithelium (HCA-7). *Br. J. Pharmacol.* **106**, 109–114 (1992).
- Egan, M. *et al.* Defective regulation of outwardly rectifying Cl⁻ channels by protein kinase A corrected by insertion of CFTR. *Nature* **358**, 581–584 (1992).
- Boucher, R.C., Stutts M.J., Knowles, M.R., Cantley, L. & Gatzky J.T. Na⁺ transport in cystic fibrosis respiratory epithelia. Abnormal basal route and response to adenylate cyclase activations. *J. clin. Invest.* **78**, 1245–1252 (1986).
- Cotton, C.U., Knowles M.R., Gatzky J.T. & Boucher R.C. Abnormal apical cell membrane in cystic fibrosis respiratory epithelium. *An in vitro electrophysiologic analysis. J. clin. Invest.* **79**, 80–85 (1987).
- Knowles, M.R., Spock, A., Fisher, N., Gatzky, J.T. & Boucher, R.C. Abnormal ion permeation through cystic fibrosis respiratory epithelium. *Science* **221**, 1067–1070 (1983).
- Tata, F. *et al.* Cloning the mouse homolog of the human cytic fibrosis transmembrane conductance regulator gene. *Genomics* **10**, 301–307 (1991).
- Van der Lugt, L., Maandag, E., te Riele, H., Laird, P.W. & Berns, A. A pgk:hprt fusion as a selectable marker for targeting of genes in mouse embryonic stem cells: disruption of the T-Cell receptor delta-chain-encoding gene. *Gene* **105**, 263–267 (1991).
- Adra, C.N., Boer, P.H. & McBurney, M.W. Cloning and expression of the mouse *pgk-1* gene and the nucleotide sequence of its promoter. *Gene* **60**, 65–74 (1987).
- Kuehn, M.R., Bradley, A., Robertson, E.J. & Evans, M.J. A potential animal model for Lesch-Nyhan syndrome through introduction of HPRT mutations into mice. *Nature* **326**, 295–298 (1987).
- Evans, M.J. Potential for genetic manipulation of mammals. *Molec. Biol. Med.* **6**, 557–565 (1989).
- Ratcliff, R. *et al.* Disruption of the cystic fibrosis transmembrane conductance regulator gene in embryonic stem cells by gene targeting. *Trans. Res.* **1**, 177–181 (1992).